Applied Physics Letters

The effect of rare-earth substitution on the Debye temperature of inorganic phosphors

Cite as: Appl. Phys. Lett. **116**, 051901 (2020); https://doi.org/10.1063/1.5142167
Submitted: 10 December 2019 . Accepted: 14 January 2020 . Published Online: 03 February 2020

Shruti Hariyani, Anna C. Duke, Thorben Krauskopf, Wolfgang G. Zeier, and Jakoah Brgoch

Applied Physics Letters ARTICLE scitation.org/journal/apl

The effect of rare-earth substitution on the Debye temperature of inorganic phosphors

Cite as: Appl. Phys. Lett. **116**, 051901 (2020); doi: 10.1063/1.5142167
Submitted: 10 December 2019 · Accepted: 14 January 2020 ·
Published Online: 3 February 2020

Shruti Hariyani,[1] Anna C. Duke,[1] Thorben Krauskopf,[2] Wolfgang G. Zeier,[2] and Jakoah Brgoch[1,a)]

AFFILIATIONS

[1]Department of Chemistry, University of Houston, Houston, Texas 77204, USA
[2]Institute of Physical Chemistry, Justus-Liebig-University Giessen, D-35392 Giessen, Germany

[a)]Author to whom correspondence should be addressed: jbrgoch@uh.edu

ABSTRACT

In the quest to predict photoluminescent efficiency in rare-earth substituted inorganic phosphors, research has shown that materials consisting of ordered, rigid crystal structures tend to possess the highest photoluminescent quantum yields. A compound's Debye temperature (Θ_D), which can be calculated using *ab initio* calculations, is an ideal proxy for quantitatively comparing structural rigidity among different inorganic compounds, allowing potentially efficient phosphors to be selected from large crystal structure databases. However, the high computational cost of these calculations limits estimating Θ_D for unsubstituted host crystal structures only. It is assumed that the low substitution concentration of the rare-earth luminescent center does not significantly influence a material's Debye temperature. This work evaluates the validity of this approximation by examining the effect of luminescent center substitution on a host structure's Θ_D. Two well-known phosphors, $(Y_{1-x}Ce_x)_3Al_5O_{12}$ $(x = 0 - 0.05)$ and $Ba_{1-\delta}Eu_\delta MgAl_{10}O_{17}$ $(\delta = 0 - 0.15)$, were synthesized with varying rare-earth concentrations, while Θ_D was computationally estimated and then determined by ultrasonic pulse-echo speed-of-sound and low-temperature heat capacity measurements. The ensuing results provide key implications for using Θ_D as a proxy for structural rigidity in substituted inorganic compounds.

Phosphor-converted light-emitting diode (LED) lights have outstanding efficiencies and long operating lifetimes, making them ideal replacements for traditional light bulbs as well as the basis of most current display technologies.[1,2] These devices operate by combining a blue-emitting LED chip and an inorganic phosphor where the LED emission is absorbed by the phosphor and then (partially or fully) down-converted to longer wavelengths.[3] The phosphors typically employed in these devices consist of a host crystal structure, such as a metal oxide or nitride, substituted with Ce^{3+} or Eu^{2+}.[4] In the search for inorganic phosphors that efficiently perform this down-conversion process, as quantified by the photoluminescent quantum yield (Φ), design rules suggest that the best materials are structurally rigid and crystallographically ordered.[5–8] Moreover, research has shown a simple method for comparing rigidity is by using a proxy such as the Debye temperature (Θ_D).[9,10] The Debye temperature can be experimentally determined from speed-of-sound or low-temperature heat capacity measurements. It can also be estimated using *ab initio* calculations combined with the quasi-harmonic Debye model.[10,11] The computational approach has the advantage that Θ_D can be determined *a priori*, allowing researchers to use high-throughput calculations to screen crystal structure databases for rigid crystal structures, thereby greatly narrowing the scope of potential phosphor hosts. One limitation of this method, however, is that these calculations are restricted to unsubstituted (pristine) host structures because calculations on rare-earth substituted phases necessitate the use of large supercells, making the process computationally demanding. A major assumption is then made that the low concentration of rare-earth in these materials minimally influences the Debye temperature.

This approximation is examined here by explicitly studying the relationship between the rare-earth concentration and Θ_D. Because most common rare-earth substituted phosphors incorporate either Ce^{3+} or Eu^{2+}, two standard phosphors that represent each category were selected for this study. The first, $Y_3Al_5O_{12}:Ce^{3+}$ ($YAG:Ce^{3+}$), illustrated in Fig. 1(a), is one of the most thoroughly studied phosphors[12,13] while the second, Eu^{2+}-substituted $BaMgAl_{10}O_{17}$ ($BAM:Eu^{2+}$), illustrated in Fig. 1(b), is also a well-established phosphor.[14,15] The diverse crystal chemistry of these materials should provide insight into the relationship between the composition, crystal structure, and resulting Θ_D as a function of rare-earth concentration.

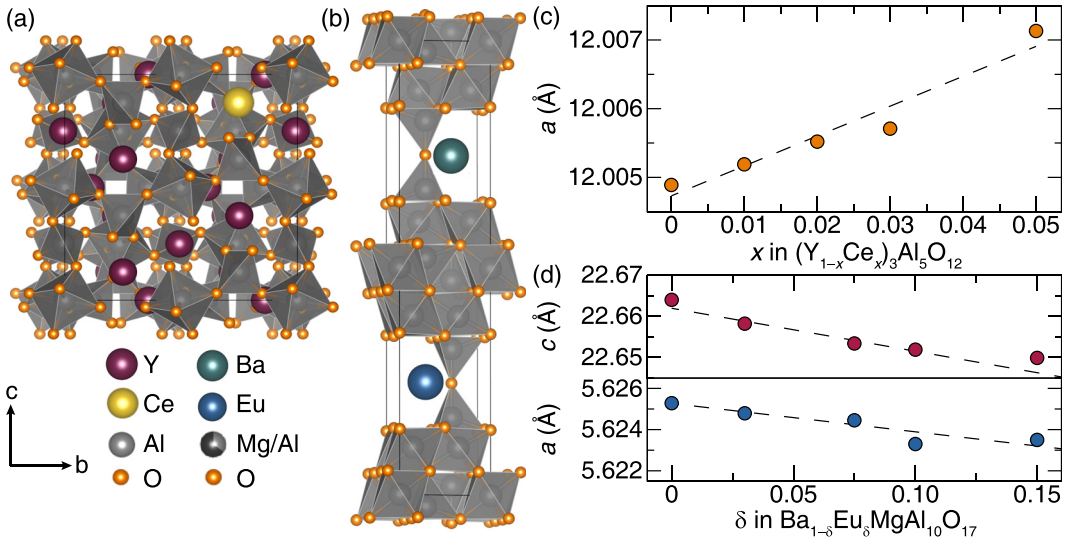

FIG. 1. (a) Crystal structure of $Y_3Al_5O_{12}$ with Ce^{3+} substituted on the Y^{3+} site. (b) $BaMgAl_{10}O_{17}$ with a Eu^{2+} atom incorporated onto the Ba^{2+} site. (c) Increasing the Ce^{3+} concentration causes an increase in the a lattice parameter, following Vegard's law. (d) Vegard's law is fulfilled as the lattice parameters decrease linearly with the increasing Eu^{2+} concentration in the a and c directions.

The Debye temperatures for these materials were first calculated employing the quasi-harmonic Debye model. In this work, Θ_D was approximated by calculating the phonon dispersion curves of each material and fitting the acoustic modes near the Γ point to obtain values of the transverse (v_T) and longitudinal (v_L) velocities. The mean velocity ($\langle v \rangle$) was then determined following Eq. (1), which was then used to calculate Θ_D following Eq. (2), where n_a is the number of atoms per formula unit, ρ is the crystallographic density, M is the molar mass, and k_B and $\hbar$ are the Boltzmann and Planck's constant, respectively. Full details of the computational procedure can be found in the supplementary material. Using this methodology, the unsubstituted YAG and BAM have Debye temperatures of 714 K and 478 K, respectively, which is in agreement with previous computational reports.[16] The incorporation of 4.2% Ce^{3+} in YAG causes a minimal rise in the compound's Θ_D to 723 K. Similarly, the Θ_D value of BAM upon 12% Eu^{2+} substitution for Ba^{2+} was determined to be 490 K. Given the low concentration of the rare-earth, equivalent to the optimized substitution percentages used experimentally, there does not appear to be a significant influence on the Debye temperature of these phases when the luminescent center is added to the host crystal structure,[12,14]

$$\langle v \rangle = \left(\frac{1}{3} \left(\frac{2}{v_T^3} + \frac{1}{v_L^3} \right) \right)^{-1/3}, \quad (1)$$

$$\Theta_D = \frac{\hbar}{k_B} \left(6\pi^2 n_a \left(\frac{N_A \rho}{M} \right) \right)^{1/3} \langle v \rangle. \quad (2)$$

To experimentally determine the effect of the substitution concentration on Θ_D, YAG:Ce^{3+} and BAM:Eu^{2+} were then synthesized with a range of rare-earth substitution concentrations. Starting from the respective metal oxides, $(Y_{1-x}Ce_x)_3Al_5O_{12}$ ($x = 0 - 0.05$) was prepared by heating the appropriate stoichiometric ratio at 1650 °C for 24 h under reducing conditions, while $Ba_{1-\delta}Eu_\delta MgAl_{10}O_{17}$ ($\delta = 0 - 0.15$) was also made in reducing conditions at 1400 °C for 4 h. Powder x-ray diffraction data were collected using Cu Kα radiation to confirm phase purity and obtain the lattice parameters of each composition using a Le Bail refinement (Fig. S1). To further verify the inclusion of the rare-earth ions and to precisely investigate the polyhedral volumes of the substitution sites, four samples of YAG:Ce^{3+} ($x = 0$, 0.01, 0.03, and 0.05) and BAM:Eu^{2+} ($\delta = 0$, 0.03, 0.10, and 0.15) were also studied by high-resolution synchrotron x-ray powder diffraction collected at the Advanced Photon Source (APS; 11-BM). These data were analyzed using Rietveld refinements as implemented within the framework of GSAS and EXPGUI (Fig. S2).[17] Figure 1(c) shows the garnet structure's a lattice parameter, and the corresponding unit cell volume increases linearly with x owing to the substitution of the larger Ce^{3+} ion for the smaller Y^{3+}.[18,19] This is in contrast to BAM:Eu^{2+}, with a decreasing a and c lattice parameter upon substitution of the smaller Eu^{2+} onto the larger Ba^{2+} site [Fig. 1(d)].[18]

Experimental determination of Θ_D via speed-of-sound and heat capacity measurements requires dense pellets. These were prepared by pressing the phase-pure polycrystalline powders into 8.5 mm pellets and sintering for 24 h in alumina crucibles under positive gas pressure (N_2 for YAG:Ce^{3+} and 5% H_2/95% N_2 for BAM:Eu^{2+}). The resulting pellets had measured densities greater than 91% (Fig. S3). The Debye temperatures were then determined first through speed-of-sound measurements by collecting the transverse (v_T) and longitudinal (v_L) velocities, provided in Figs. S4(a) and S4(c). The results, obtained following Eqs. (1) and (2), indicate that upon increasing the Ce^{3+} concentration in YAG:Ce^{3+}, the Debye temperature remains stable with $\Theta_D \approx 710$ K [Figs. S4(a) and S4(b)]. This is likely because substituting the similar sized, isovalent Ce^{3+} onto the Y^{3+} site does not significantly influence the local crystal chemistry, which minimizes the changes in the phonon modes that influence Θ_D. Θ_D of BAM:Eu^{2+}, determined from the speed-of-sound measurements, remains steady (530 K) at low substitution concentrations and then slightly increases to 600 K at higher Eu^{2+} concentrations [Figs. S4(c) and S4(d)]. The

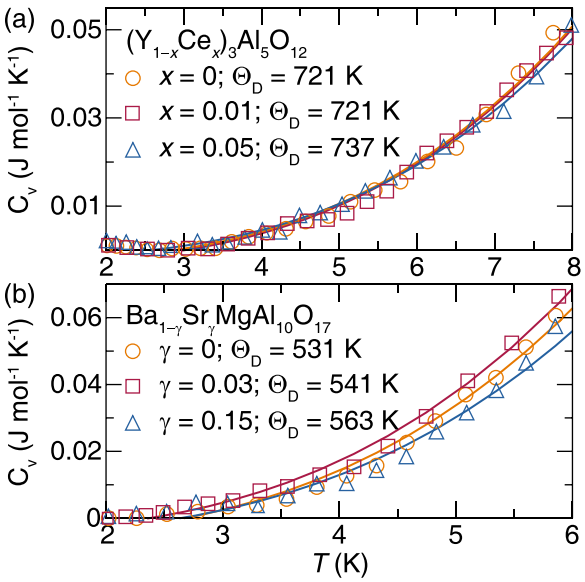

FIG. 2. Low temperature heat capacity measurements for (a) $(Y_{1-x}Ce_x)_3Al_5O_{12}$ ($x = 0$, 0.01, and 0.05) and (b) $Ba_{1-\gamma}Sr_\gamma MgAl_{10}O_{17}$ ($\gamma = 0$, 0.03, and 0.15) with Debye model fittings in the colors with respect to the sample doping concentration.

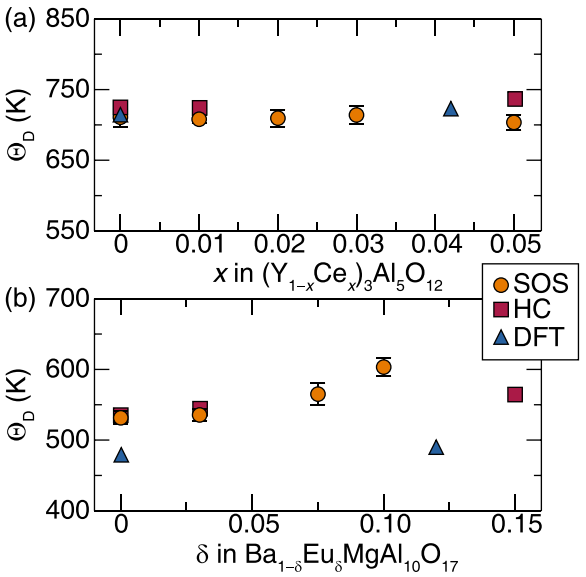

FIG. 3. (a) Debye temperatures collected for $(Y_{1-x}Ce_x)_3Al_5O_{12}$ ($x = 0$–0.05) and (b) $Ba_{1-\delta}(Eu/Sr)_\delta MgAl_{10}O_{17}$ ($\delta = 0 - 0.15$) from speed-of-sound measurements (orange circle), low temperature heat capacity measurements (red square), and *ab initio* calculations (blue triangle).

increase in measured Θ_D is likely because the substitution of the smaller, chemically harder Eu^{2+} ion for the softer Ba^{2+} ion enhances structural rigidity and therefore Θ_D. This mirrors the behavior of previously explored systems, such as $Ba_2(Y_{1-x}Lu_x)_5B_5O_{17}$:$Ce^{3+}$ and $Ba_{2-x}Sr_xSiO_4$:Ce^{3+}.[20,21] However, there is only an overall 10% change, indicating that the change to the material's Θ_D is relatively minor even at high rare-earth substitution.

There are multiple experimental methods to measure a material's Θ_D; thus, a second approach was sought to corroborate the speed-of-sound results. Low-temperature heat capacity data were accordingly collected from 2 K to 12 K. The data were fit following the Debye T^3 law, provided in Eq. (3), where N is Avogadro's number multiplied by the number of atoms in one formula unit, k_B is the Boltzmann constant, and T is the sample temperature,[22]

$$C_v \approx \frac{12Nk_B\pi^4}{5}\left(\frac{T}{\Theta_D}\right)^3. \quad (3)$$

The heat capacity of YAG:Ce^{3+} for $x = 0$, 0.01, and 0.05 was measured and the data fit from 2 K to 8 K to extract Θ_D. As shown in Fig. 2(a), upon increasing Ce^{3+}, Θ_D remains relatively unchanged, confirming that the presence of Ce^{3+} has little effect on Θ_D of YAG:Ce^{3+}. Examining the heat capacity data of BAM:Eu^{2+} was decidedly more complicated. Initial low temperature heat capacity measurements on BAM:Eu^{2+} showed Eu^{2+} magnetic transitions at <4 K despite the dilute concentration of the rare-earth (Fig. S5), making fitting the data following Eq. (3) unfeasible.[23] Therefore, a series of Sr-substituted BAM was pursued instead due to the similar ionic radii of Sr^{2+} ($r_{9\text{-coord}} = 1.31$ Å) to Eu^{2+} ($r_{9\text{-coord}} = 1.30$ Å), isovalency, and diamagnetic response of Sr^{2+}.[24] These powders were prepared following the same synthesis and densification process (Fig. S1). The resulting heat capacity measurements provided high-quality data that could be reliably fit to obtain Θ_D. For BAM:Sr^{2+}, fitting from 2 K to 6 K follows a similar trend as observed from speed-of-sound measurements with a minor increase from 531 K to 563 K upon increasing $\gamma = 0$ to $\gamma = 0.15$.

The two experimental approaches for determining Θ_D as well as the computational values determined from *ab initio* calculations demonstrate reasonable agreement among the different methods (Fig. 3).

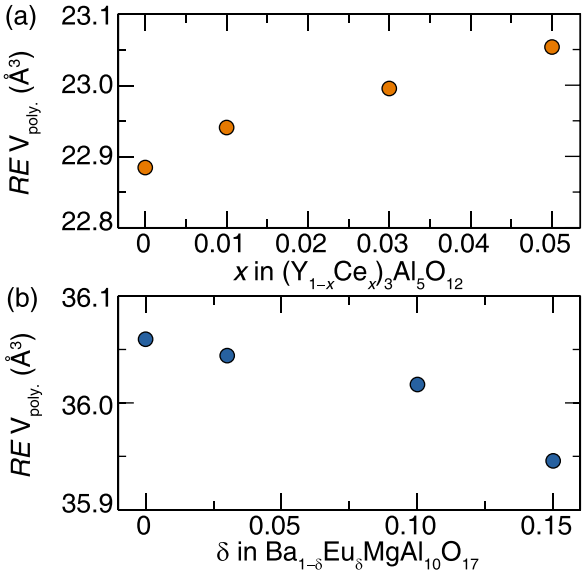

FIG. 4. (a) Refined substitution site polyhedral volume upon Ce^{3+} substitution in YAG. (b) Refined substitution site polyhedral volume upon Eu^{2+} substitution in BAM.

Although there is a small spread in Θ_D, this is anticipated given the nuances associated with determining the Debye temperature. In the case of YAG:Ce^{3+}, the measured Θ_D ranges between 703 K and 737 K across the rare-earth substitution range, while the computationally determined Θ_D of the pristine host is 714 K and 723 K for the substituted structure. These differences are insignificant and demonstrate that the substitution of Ce^{3+} ($0 \leq x \leq 0.05$) has little effect on the Debye temperature and by proxy the structural rigidity of yttrium aluminum garnet. Such a negligible change in Θ_D for YAG is somewhat expected. For example, it is well-known that the substitution of Ce^{3+} on the Y^{3+} site in YAG:Ce^{3+} leads to only minor modifications in the crystal structure including a small change in the unit cell volume upon substitution.[19] This is further supported by analyzing the change in the polyhedron bond length and volume of the rare-earth substitution site as a function of the nominally loaded concentration (Table S3). Figure 4(a) shows that there is a small but steady increase in the polyhedral volume as the concentration of Ce^{3+} increases. This is driven largely by the fact that Y^{3+} ($r_{8\text{-coord}} = 1.02$ Å) is not only very similar in size to Ce^{3+} ($r_{8\text{-coord}} = 1.14$ Å) but also the garnet structure has a pair of robust interpenetrating Y − O and Al−O networks that form a double-gyroid structure, making the structure resistant to significant changes even upon elemental substitution.[19] As a result, only minor changes in the phonon spectrum are anticipated upon incorporation of Ce^{3+}, which is in agreement with the unvarying experimental Debye temperature determined here.

The Debye temperatures for BAM:Eu^{2+} show slightly less agreement, but an overall similar trend. As plotted in Fig. 3(b), increasing the substitution concentration in BAM tends to yield a minor increase in Θ_D. At low substitution values, Θ_D is approximately 535 K, which is in reasonable agreement with the computational approximation ($\Theta_D = 482$ K). Upon substitution, the experimentally measured Debye temperature increases to a maximum of 603 K based on the speed of sound measurements (when $\delta = 0.075$) and 563 K using heat capacity measurements (when $\delta = 0.15$). The origin of the response in Eu^{2+} substituted BAM is slightly different and to some extent unanticipated. Analyzing BAM as a function of rare-earth concentration shows that when $\delta < 0.05$, the crystal structure and Debye temperature remain relatively static, which is understandable based on the low substitution concentration even though the ionic radii of Ba^{2+} ($r_{9\text{-coord}} = 1.47$ Å) and Eu^{2+} ($r_{9\text{-coord}} = 1.30$ Å) are 12% different. Increasing the Eu^{2+} concentration further causes the Debye temperature to increase slightly following the decrease in the unit cell volume as refined from synchrotron x-ray powder diffraction. The smaller unit cell and shorter bond lengths in the [(Ba/Eu)O_9] polyhedra, resulting from the difference in the atomic radii between Ba^{2+} and Eu^{2+}, lead to a slight stiffening of the crystal structure as observed here based on the increase in Θ_D. This phenomenon can also been observed in other systems as well.[25–27] However, analyzing the changes in the [(Ba/Eu)O_9] units shows that the average polyhedral volume only slightly decreases, changing by <1% even up to $\delta = 0.15$. Given the size difference between Ba^{2+} and Eu^{2+}, a large change was expected; thus, further investigation may be necessary to explicitly examine the coordination environment of the rare-earth in BAM:Eu^{2+} such as using a pair distribution function analysis or similar local structure technique. Nevertheless, it is important to note that the most prominent change in the experimentally measured Debye temperatures of BAM occurs when Eu^{2+} is >10–15 mol. %, which is ≈3 times the rare-earth concentration examined for YAG. Therefore, the minor effect of rare-earth substitution on the host structure may only be observed at elevated concentrations. The Debye temperature remains generally invariant as a function of rare-earth substitution, particularly at relatively low substitution concentrations commonly employed in most phosphors.

In summary, $(Y_{1-x}Ce_x)_3Al_5O_{12}$ ($x = 0$–0.05) and $Ba_{1-\delta}Eu_\delta MgAl_{10}O_{17}$ ($\delta = 0$–0.15) were prepared and their Debye temperatures were experimentally determined using speed-of-sound and low-temperature heat capacity measurements and computationally approximated using density functional theory (DFT). In combination, these results prove that there is a minimal change in the host's Debye temperature across a range of rare-earth substitution concentrations. Comparing changes in the crystal structure and the substitution site polyhedral volume upon increasing the rare-earth concentration suggests that incorporation of rare-earth ions in host lattices does not lead to significant deviations from the unsubstituted phase, causing the value of Θ_D to be largely unaffected. This is particularly true for the relatively low substitution concentrations (often less than 5 mol. %) used in most phosphors. Moreover, the DFT calculated Θ_D is within about ±5% of the average experimentally measured Θ_D. This work, therefore, further strengthens the case for using the calculated Θ_D of an unsubstituted host structure as a proxy for structural rigidity, especially for low rare-earth substitution concentrations, and therefore as a tool to predict luminescence efficiency in inorganic phosphors.

See the supplementary material for the complete experimental workup including synthesis, refinement details, and speed-of-sound and low temperature heat capacity measurement procedures. Additionally, the computational methodology including structure optimization and calculation of the phonon dispersion curves using density functional theory is outlined in the supplementary material.

The authors thank the National Science Foundation (Nos. DMR 18-47701 and CER 19-11311) as well as the R. A. Welch Foundation (No. E-1981) for supporting this work. This research used the Maxwell/Opuntia/Sabine cluster(s) operated by the Research Computing Data Core at the University of Houston. Support for this work was also provided by resources of the uHPC cluster managed by the University of Houston and acquired through NSF Award No. 15-31814. This work used the resources available through the 11-BM beamline at the Advanced Photon Source, an Office of Science User Facility operated for the U.S. Department of Energy (DOE) Office of Science by Argonne National Laboratory, under Contract No. DE-AC02-06CH11357.

REFERENCES

[1]A. Rapaport, J. Milliez, M. Bass, A. Cassanho, and H. Jenssen, J. Disp. Technol. **2**(1), 68 (2006).
[2]H. A. Höppe, Angew. Chem. Int. Ed. **48**(20), 3572 (2009).
[3]M. F. J. L. Leano, Jr. and R. Lio, ECS J. Solid State Sci. Technol. **7**(1), R3111 (2018).
[4]N. C. George, K. A. Denault, and R. Seshadri, Annu. Rev. Mater. Res. **43**(1), 481 (2013).
[5]A. F. Pozharskii, A. R. Katritzky, and A. Soldatenkov, *Heterocycles in Life and Society: An Introduction to Heterocyclic Chemistry, Biochemistry and Applications*, 2nd ed. (John Wiley & Sons, Hoboken, NJ, 2011).
[6]J. D. Furman, B. C. Melot, S. J. Teat, A. A. Mikhailovsky, and A. K. Cheetham, Phys. Chem. Chem. Phys. **13**(17), 7622 (2011).

[7]K. A. Denault, J. Brgoch, M. W. Gaultois, A. Mikhailovsky, R. Petry, H. Winkler, S. P. DenBaars, and R. Seshadri, Chem. Mater. **26**(7), 2275 (2014).
[8]L. He, Z. Song, Q. Xiang, Z. Xia, and Q. Liu, J. Lumin. **180**, 163 (2016).
[9]K. A. Denault, J. Brgoch, S. D. Kloß, M. W. Gaultois, J. Siewenie, K. Page, and R. Seshadri, ACS Appl. Mater. Interfaces **7**(13), 7264 (2015).
[10]J. Brgoch, S. P. DenBaars, and R. Seshadri, J. Phys. Chem. C **117**(35), 17955 (2013).
[11]F. Peng, H. Fu, and X. Yang, Physica B **403**(17), 2851 (2008).
[12]V. Bachmann, C. Ronda, and A. Meijerink, Chem. Mater. **21**(10), 2077 (2009).
[13]M. Moszyński, T. Ludziejewski, D. Wolski, W. Klamra, and L. O. Norlin, Nucl. Instrum. Methods Phys. Res., Sect. A **345**(3), 461 (1994).
[14]K.-B. Kim, Y.-I. Kim, H.-G. Chun, T.-Y. Cho, J.-S. Jung, and J.-G. Kang, Chem. Mater. **14**(12), 5045 (2002).
[15]Y. Wang, X. Xu, L. Yin, and L. Hao, J. Am. Ceram. Soc. **93**(6), 1534 (2010).
[16]Z. Huang, J. Feng, and W. Pan, Solid State Sci. **14**(9), 1327 (2012).
[17]B. H. Toby, J. Appl. Crystallogr. **34**(2), 210 (2001).
[18]E—A. Zen, Am. Miner. **41**(5–6), 523 (1956).
[19]N. C. George, A. J. Pell, G. Dantelle, K. Page, A. Llobet, M. Balasubramanian, G. Pintacuda, B. F. Chmelka, and R. Seshadri, Chem. Mater. **25**(20), 3979 (2013).
[20]M. Hermus, P.-C. Phan, A. C. Duke, and J. Brgoch, Chem. Mater. **29**(12), 5267 (2017).
[21]X. Ji, J. Zhang, Y. Li, S. Liao, X. Zhang, Z. Yang, Z. Wang, Z. Qiu, W. Zhou, L. Yu, and S. Lian, Chem. Mater. **30**(15), 5137 (2018).
[22]T. Krauskopf, C. Pompe, M. A. Kraft, and W. G. Zeier, Chem. Mater. **29**(20), 8859 (2017).
[23]W. B. Jiang, M. Smidman, W. Xie, J. Y. Liu, J. M. Lee, J. M. Chen, S. C. Ho, H. Ishii, K. D. Tsuei, C. Y. Guo, Y. J. Zhang, H. Lee, and H. Q. Yuan, Phys. Rev. B **95**(2), 024416 (2017).
[24]R. D. Shannon, Acta Crystallogr., Sect. A **A32**(5), 751 (1976).
[25]Y. B. Losovyj, I. N. Yakovkin, H.-K. Jeong, D. Wisbey, and P. A. Dowben, J. Phys.: Condens. Matter **16**(26), 4711 (2004).
[26]M. F. Bakar and A. K. Yahya, J. Alloys Compd. **490**(1), 358 (2010).
[27]A. K. Yahya and R. Abd-Shukor, Supercond. Sci. Technol. **11**(2), 173 (1998).